Article type : Original Article

Aquaporin 9 Induction in Human iPSC-derived Hepatocytes Facilitates Modeling of Ornithine Transcarbamylase Deficiency

Alexander Laemmle[1,2,3], Martin Poms[4], Bernadette Hsu[1], Mariia Borsuk[3], Véronique Rüfenacht[5], Joshua Robinson[1,6,7,8], Martin C. Sadowski[9], Jean-Marc Nuoffer[2,3], Johannes Häberle[5,10*], Holger Willenbring[1,11,12*]

[1]Eli and Edythe Broad Center of Regeneration Medicine and Stem Cell Research, University of California San Francisco, CA 94143, USA

[2]Department of Pediatrics, University Children's Hospital, Bern, Switzerland

[3]University Institute of Clinical Chemistry, University of Bern, Bern, Switzerland

[4]Division of Clinical Chemistry and Biochemistry, University Children`s Hospital Zurich, Switzerland

[5]Division of Metabolism and Children`s Research Center (CRC), University Children`s Hospital, Zurich, Switzerland

[6]Center for Reproductive Sciences, University of California San Francisco, CA 94143, USA

[7]Department of Obstetrics, Gynecology, and Reproductive Sciences, University of California San Francisco, CA 94143, USA

[8]Department of Pediatrics, Medical Genetics, University of California San Francisco, CA 94143, USA

[9]Institute of Pathology, University of Bern, Bern, Switzerland

[10]Zurich Center for Integrative Human Physiology, University of Zurich, Zurich, Switzerland

[11]Department of Surgery, Division of Transplant Surgery, University of California San Francisco, CA 94143, USA
[12]Liver Center, University of California San Francisco, CA 94143, USA
*Shared last authorship
alexander.laemmle@insel.ch
martin.poms@kispi.uzh.ch
bernadette.hsu@ucsf.edu
mariia.borsuk@students.unibe.ch
veronique.ruefenacht@kispi.uzh.ch
joshua.robinson@ucsf.edu
martin.sadowski@pathology.unibe.ch
jean-marc.nuoffer@insel.ch
johannes.haeberle@kispi.uzh.ch
holger.willenbring@ucsf.edu

Keywords

Liver disease modeling

Induced pluripotent stem cells

Urea cycle disorders

Ammonia detoxification

Ureagenesis

Footnote page

Contact Information

Corresponding author: Alexander Laemmle

Address: University Institute of Clinical Chemistry and Department of Pediatrics; Kinderklinik H524, Freiburgstrasse 15, 3010 Bern, Switzerland

Phone: +41 31 632 95 44

E-mail: alexander.laemmle@insel.ch

List of Abbreviations

AFP, alpha-fetoprotein; ALB, albumin; AQP9, aquaporin 9; ARG1, arginase 1; ASL, argininosuccinate lyase; ASS, argininosuccinate synthetase; CPS1, carbamoylphosphate synthetase 1; GEO, gene expression omnibus; gDNA, genomic DNA; HCM, hepatocyte culture medium; hESCs, human embryonic stem cells; hiPSCs, human induced pluripotent stem cells; hiPSC-Heps, hiPSC-derived hepatocytes; LDL, low-density lipoprotein; mRNA, messenger RNA; OTC, ornithine transcarbamylase; OTCD, OTC deficiency; PHHs, primary human hepatocytes; UCD, urea cycle disorder; UCEs, urea cycle enzymes; $^{15}NH_4Cl$, [^{15}N]ammonium chloride

Financial Support

AL received funding from the "Novartis Stiftung für Medizinisch-Biologische Forschung" (Research fellowship, Nr. 15B086), from the "Fondazione Ettore and Valeria Rossi" and from the "Batzenbär-Stiftung des Inselspitals". Urea cycle disorders research in Zurich is supported by the Swiss National Science Foundation (grant 320030_176088 to JH). HW was funded by UH3 TR000487 and P30 DK26743 from the National Institutes of Health and DISC2-10088 from the California Institute for Regenerative Medicine.

Abstract

Background & Aims: Patient-derived human induced pluripotent stem cells (hiPSCs) differentiated into hepatocytes (hiPSC-Heps) have facilitated the study of rare genetic liver diseases. Here, we aimed to establish an *in vitro* liver disease model of the urea cycle disorder ornithine transcarbamylase deficiency (OTCD) using patient-derived hiPSC-Heps. *Approach & Results:* Before modeling OTCD, we addressed the question of why hiPSC-Heps generally secrete less urea than adult primary human hepatocytes (PHHs). Since hiPSC-Heps are not completely differentiated and maintain some characteristics of fetal PHHs, we compared gene expression levels in human fetal and adult liver tissue to identify genes responsible for reduced urea secretion in hiPSC-Heps. We found lack of aquaporin 9 (AQP9) expression in fetal liver tissue as well as in hiPSC-Heps, and showed that forced expression of AQP9 in hiPSC-Heps restores urea secretion and normalizes the response to ammonia challenge by increasing ureagenesis. Furthermore, we proved functional ureagenesis by challenging AQP9-expressing hiPSC-Heps with ammonium chloride labeled with the stable isotope [^{15}N] ($^{15}NH_4Cl$) and by assessing enrichment of [^{15}N]-labeled urea. Finally, using hiPSC-Heps derived from patients with OTCD, we generated a liver disease model that recapitulates the hepatic manifestation of the human disease. Restoring OTC expression—together with AQP9—was effective in fully correcting OTC activity and normalizing ureagenesis as assessed by $^{15}NH_4Cl$ stable-isotope challenge. *Conclusion:* Our results identify a critical role for AQP9 in functional urea metabolism and establish the feasibility of *in vitro* modeling of OTCD with hiPSC-Heps. By facilitating studies of OTCD genotype/phenotype correlation and drug screens, our model has potential for improving the therapy of OTCD.

Human induced pluripotent stem cell (hiPSC)-derived hepatocytes (hiPSC-Heps) generated from patients with genetically encoded liver diseases have been successfully used to model liver diseases *in vitro*, leading to a better understanding of disease mechanisms and the identification of new therapeutic agents (1).

Urea cycle disorders (UCDs) are a group of eight inborn errors of metabolism that can be life threatening and for which treatment options are limited (2, 3). Urea is the waste product arising from ammonia (NH_4^+) detoxification in the urea cycle, which consists of five urea cycle enzymes (UCEs) located in mitochondria—carbamoylphosphate synthetase 1 (CPS1) and ornithine transcarbamylase (OTC)—or cytoplasm—argininosuccinate synthetase (ASS), argininosuccinate lyase (ASL) and arginase 1 (ARG1)—of hepatocytes (Figure 1A). An additional UCD is caused by deficiency of N-acetylglutamate synthase (NAGS), which is required for CPS1 activation. The two remaining UCDs are caused by defects in mitochondrial citrin and ornithine transporters, leading to citrin deficiency and hyperornithinemia-hyperammonemia-homocitrullinuria syndrome, respectively.

To date, only ARG1 deficiency, ASS deficiency and citrin deficiency have been modeled using hiPSC-Heps (4-6). A hiPSC-Hep-based model of OTC deficiency (OTCD) has yet to be reported. Although OTCD is the most common UCD (7), resulting in substantial clinical experience, its prognosis is unpredictable because disease onset and severity are affected by a large number of different mutations (8) and variable effects of X-chromosome inactivation in women (9). The current treatment, consisting of low-protein diet and supplementation of essential amino acid mixtures (10), is challenging and often fails to prevent adverse outcomes in patients (11), leading to a high mortality rate (12). A faithful disease model would help to better understand the relationship between gene defect and disease manifestation, allowing prediction of the disease course in individual patients, and could be used to develop novel therapeutics.

A potential reason for the lack of a hiPSC-Hep model of OTCD is that ureagenesis is generally low in hiPSC-Heps, both in hiPSC-Heps derived from normal controls and in hiPSC-Heps in which the genetic defect causing the UCD was corrected (4-6, 13). This functional deficiency is consistent with the general notion that hiPSC-Heps generated with current protocols are not as

differentiated as adult primary human hepatocytes (PHHs) but retain some fetal characteristics (14).

We overcame this roadblock by identifying lack of expression of aquaporin 9 (AQP9), a membrane channel protein that mediates passage of water, glycerol and urea (15, 16), as the reason for low ureagenesis in hiPSC-Heps. Taking advantage of this insight to establish functional urea metabolism in hiPSC-Heps, we developed an *in vitro* model of genotype-specific manifestation of OTCD.

Materials and Methods

Patients

Written informed consent was obtained from all study subjects. These studies were approved by the local ethics committee in Bern, Switzerland (project ID: 2020-02979).

Reprogramming of Fibroblasts into hiPSCs and Directed Differentiation of hiPSCs into hiPSC-Heps

hiPSCs were generated and cultured as previously described (17). Hepatocyte differentiation of hiPSCs recapitulating critical stages of development was performed as we previously described for Ctrl_1 line (18) (for details see Supporting Methods).

Cell Culture and Origin of PHHs

PHHs were purchased from BioIVT (catalog number M00995-P; lot numbers BVI, FLO and JFC). Biological replicates were generated using all three PHH lots. Cells were plated on rat tail collagen type I-coated plates at a density of 6.0 x 10^4 cells/cm^2 in Dulbecco`s minimum essential medium (DMEM) supplemented with 10% fetal bovine serum, glutaMax™, 50 U/mL penicillin, 50 µg/mL streptomycin, and 1 µmol/L dexamethasone and insulin. After overnight culture, the medium was replaced by serum-free Williams E medium containing the same concentrations of penicillin/streptomycin, dexamethasone and insulin.

Urea Assay and Albumin ELISA

To assess cellular urea and/or albumin secretion we collected cell culture supernatants at the indicated time-points (usually after 24 hours), centrifuged them at 700 x g for 5 minutes at 4°C and either directly measured or stored samples at -80°C and later determined urea and/or albumin concentration with the Quantichrom Urea Assay Kit (Bioassay Systems) and/or Albumin ELISA (Bethyl Laboratories). The absolute amount of secreted urea and/or albumin was expressed in pg/cell/24 hours.

Quantitative PCR

For RNA isolation we used the RNAeasy Mini Kit (Qiagen). All samples were treated with DNAse. Reverse transcription was performed using qScript cDNA Supermix (Quanta

Biosciences). qPCR was performed using a SYBR Green Supermix (Affymetrix) on an Applied Biosciences ViiA7 Real-Time PCR System (Thermo Fisher Scientific). Reactions were performed in triplicate, and expression was normalized to *GAPDH* or *18S* gene expression and quantified using the ΔΔCt method. Primers are listed in Supporting Methods.

Western Blot

Western blot was performed using 10% SDS-PAGE as described previously (19). Further details and antibodies are given in Supporting Methods.

Immunofluorescence

Immunofluorescence imaging was performed as described previously (20). Further details and antibodies are given in Supporting Methods.

Relative mRNA Expression in Liver Tissue and in hiPSC-Heps

A microarray data set previously published by Bonder et al. (21)—deposited in the NCBI GEO database under accession number GSE61279—was analyzed for relative messenger RNA (mRNA) expression of *AQP9* and other enzymes and transporters involved in ammonia detoxification and urea metabolism in fetal and adult human liver tissue.

In addition, expression of these genes in hiPSC-Heps and PHHs was assessed in four additional datasets deposited in the GEO database (22-25). More information about these datasets is given in Supporting Methods.

Lentiviral Transduction

Lentiviral vectors were custom-designed at and purchased from VectorBuilder. All lentiviral vectors had viral titers of at least 5 x 10^8 TU/mL and expressed AQP9 (vector ID: VB180418-1015mqd), OTC (vector ID: VB191009-1069yvq) or GFP (vector ID: VB180418-1016dym). The genes were under the control of the ubiquitously active EF1A promoter. Vector details are available at https://en.vectorbuilder.com. Cells were transduced on day 18 of the hiPSC-Heps differentiation protocol using a multiplicity of infection of 20 in hepatocyte culture medium (HCM) (Lonza; for details see Supporting Methods) supplemented with 10 µg/ml polybrene. After overnight transduction, cells were washed with PBS and HCM was added.

$^{15}NH_4Cl$ Challenge and Isotopic [^{15}N]Urea Enrichment

One molar aqueous stock solutions of NH_4Cl and $^{15}NH_4Cl$ (Sigma Aldrich) were prepared and filter-sterilized prior to use in cell cultures at working concentrations of 0, 1, 2 and 10 mM. Samples of the cell culture supernatants were taken at 2 hours and 24 hours. Isotopic [^{15}N]urea enrichment and semi-quantitative amino acid concentrations were measured by adjustment for cell culture supernatants using a previously described method (26).

Ornithine Transcarbamylase Activity Assay

An adapted version of a previously established OTC activity assay (27) was performed to determine OTC activity in cell culture lysates. Briefly, 25 to 50 μg of whole cell lysates were used to assess OTC activity. The substrates ornithine and carbamoylphosphate were added in excess to the lysates. Citrulline, which is produced in the OTC enzyme reaction, was measured spectrophotometrically after a color reaction with diacetylmonoxim/antipyrin/Fe. The intensity of the absorption is proportional to the amount of produced citrulline, which is proportional to the OTC enzyme activity.

Statistical Analysis

All experiments were repeated at least twice with a minimum of two biological replicates. Student *t* test or ordinary one-way ANOVA was used to compare groups, with significance set at $p < 0.05$. Data are expressed as mean and error bars represent standard error of mean (SEM).

Results

Urea Metabolism is Impaired in hiPSC-Heps

Although hiPSC-Heps express many functions of mature adult PHHs, they also exhibit characteristics of immature fetal PHHs, including reduced capacity to secrete urea (14). Therefore, as the first step toward using patient-derived hiPSC-Heps to create an *in vitro* model of OTCD, we investigated ammonia detoxification and urea metabolism in hiPSC-Heps derived from normal controls. We generated four hiPSC lines from normal controls and differentiated them into hiPSC-Heps (Ctrl_1-4 hiPSC-Heps) using our step-wise hepatocyte differentiation protocol (Supporting Fig. 1A; for details see Supporting Methods and (18)). Ctrl_1 hiPSC-Heps showed characteristic hepatocyte morphology (Supporting Fig. 1A) and well-developed hepatocyte functions, including albumin secretion (Supporting Fig. 1B), CYP3A4-mediated drug metabolism (Supporting Fig. 1C), low-density lipoprotein (LDL) receptor-mediated LDL uptake (Supporting Fig. 1D) and *ALB* and *HNF4A* mRNA expression (Supporting Fig. 1E). However, Ctrl_1-4 hiPSC-Heps showed significantly lower urea secretion than PHHs (Figure 1B). Analysis of mRNA and protein expression in Ctrl_1 hiPSC-Heps showed that the five UCEs were expressed, some at similar levels and some at lower levels than in PHHs (Figure 1C and D). As expected, UCE expression in hiPSCs was very low or absent. Immunofluorescent staining of the two most abundant UCEs CPS1 and OTC showed mitochondrial localization as expected (Figure 1E and Supporting Fig. 1F).

These results confirmed that hiPSC-Heps secrete lower amounts of urea than PHHs. The overall reduction in UCE expression likely contributed to the decreased urea secretion found in hiPSC-Heps, but the extent to which urea secretion was impaired in hiPSC-Heps suggested the contribution of factors beyond the UCEs.

Urea Metabolism is Impaired in hiPSC-Heps Due to Lack of AQP9

Considering that hiPSC-Heps maintain many characteristics of fetal hepatocytes, e.g., alpha-fetoprotein (*AFP*) mRNA expression (Supporting Fig. 1E), we reasoned that comparing mRNA expression in human fetal and adult liver tissue will reveal genes responsible for low urea secretion in hiPSC-Heps. For this, we analyzed published mRNA expression profiling of 14 fetal and 92 adult human liver tissue samples (GSE62179) (21) (Figure 2A). mRNA expression of the five UCEs, NAGS and two mitochondrial transporters (encoded by *SLC25A13* and *SLC25A15*) involved in ureagenesis showed little variation between fetal and adult human liver tissue samples (Figure 2A). However, expanding the analysis revealed *AQP9* as one of the most differentially expressed genes in GSE62179 ($p < 1.0E-07$), exhibiting higher abundance in adult (≥ 70-fold higher expression) than in fetal liver (Figure 2A).

AQP9 is located in the hepatocyte plasma membrane and is required for urea transport across this membrane (28, 29). As in human fetal liver, comparison to PHHs showed that *AQP9* expression was lacking in hiPSC-Heps, as evidenced not only by analysis of hiPSC-Heps generated with our current protocol (Figure 2B) but also hiPSC-Heps generated with a previous version of our protocol (GSE52309) (25) or three additional gene expression profiles of hiPSC-Heps generated in other laboratories (22-24) (Supporting Fig. 2A and Supporting Methods).

If lack of AQP9 expression was contributing to low ureagenesis in hiPSC-Heps, urea should be accumulating intracellularly. Indeed, intracellular urea levels were higher in hiPSC-Heps than in PHHs (Figure 2C). Moreover, lentiviral expression of AQP9 in hiPSC-Heps (Supporting Fig. 2B) restored urea secretion (Figure 2B and D) and decreased intracellular urea levels (Figure 2E). To further study ammonia detoxification and urea metabolism in hiPSC-Heps, we challenged the cells with ammonium chloride (NH_4Cl). In contrast to PHHs, hiPSC-Heps failed to increase urea secretion in response to NH_4Cl (Supporting Fig. 2C). However, lentiviral AQP9 expression in hiPSC-Heps normalized the response to NH_4Cl challenge, i.e., increased urea secretion (Figure 2F). Taken together, our findings show that hiPSC-Heps generated with current protocols lack AQP9 expression and its restoration normalizes basal and ammonia-induced urea secretion.

AQP9 Expression Normalizes Response of hiPSC-Heps to Ammonia Challenge

To further characterize ammonium detoxification and urea metabolism and to demonstrate functional ureagenesis in AQP9-expressing hiPSC-Heps, we challenged the cells with NH_4Cl labeled with the stable isotope [^{15}N] ($^{15}NH_4Cl$) to measure the enrichment of secreted [^{15}N]-labeled urea (Figure 3A and B). If ureagenesis is functional, three different isotopes of urea are detectable after such a challenge: non-labeled urea, mono-labeled urea and double-labeled urea. Mono-labeled urea receives the labeled [^{15}N]-atom from NH_4^+ in carbamoylphosphate or aspartate. Double-labeled urea receives one [^{15}N]-atom from carbamoylphosphate and one [^{15}N]-atom from aspartate (Figure 3A). Challenging the AQP9-expressing hiPSC-Heps with 1, 2 or 10 mM of $^{15}NH_4Cl$ led to an increase of [^{15}N]-mono- and double-labeled urea when compared to untreated (0 mM) cells, which demonstrated functional ureagenesis (Figure 3B).

Further analysis of amino acid concentrations in the cell culture supernatants revealed glutamine and alanine as the two most abundant amino acids (levels between approximately 700 μM and 2200 μM; Supporting Fig. 3). After hiPSC-Heps were challenged with 1 mM of NH_4Cl for 24 hours, glutamine concentrations increased by a factor of approximately 1.6 (from 700 μM to 1200 μM; Supporting Fig. 3), consistent with glutamine acting as an ammonia-scavenging back-up system as observed *in vivo* (30).

Taken together, these results show that expression of AQP9 in hiPSC-Heps normalized the reaction to ammonia challenge, i.e., ammonia conversion into urea and its secretion out of the cells into the culture medium. In addition to demonstrating functional ureagenesis, these results show physiological ammonia flux into urea and amino acid changes in AQP9-expressing hiPSC-Heps.

Generation of hiPSC-Heps from Patients with Ornithine Transcarbamylase Deficiency

We generated hiPSC lines from fibroblasts of two patients who died from OTCD (31). Analysis of *OCT3/4* and *NANOG* mRNA (Supporting Fig. 4A) and OCT3/4 and SSEA4 protein expression (Supporting Fig. 4B) confirmed the cells' pluripotency. One patient, designated OTCD_1, was male and died in the neonatal period. Mutational analysis of the patient`s fibroblasts revealed a previously described hemizygous mutation in the *OTC* gene, which is located on the X chromosome (exon 6; c.548A>G (p.Tyr183Cys)) (32). We confirmed the presence of the mutation in hiPSC-Heps generated from the patient's fibroblasts (Figure 4A). Due to the X-chromosomal inheritance of OTCD, male patients often suffer from a fatal disease course; in female patients, the

disease course is affected by X inactivation and therefore more variable. The second patient (OTCD_2) was female and developed fatal acute liver failure at the age of six years suggesting skewed X inactivation strongly favoring the mutated allele. She had a previously described heterozygous stop mutation in the *OTC* gene (exon 3; c.274C>T (p.Arg92*) (33), which we confirmed to be present heterozygously in genomic DNA (gDNA) in hiPSC-Heps (Figure 4A). Analysis of *OTC* mRNA in hiPSC-Heps revealed complete inactivation of the normal allele of the *OTC* gene, leading to only the mutated allele being expressed, which is in line with the skewed X inactivation found in the patient (Figure 4A and B).

Differentiation of OTCD hiPSCs using our standard protocol (Supporting Fig. 1A) produced hiPSC-Heps with hepatocyte-specific morphology (Figure 4C), albumin secretion (Supporting Fig. 5A) and mRNA (Supporting Fig. 5B) and protein (Supporting Fig. 5C) expression.

Modeling Ornithine Transcarbamylase Deficiency with Patient-derived hiPSC-Heps

OTCD_1 and OTCD_2 hiPSC-Heps transduced with lentiviruses expressing AQP9 showed significantly reduced urea secretion compared to AQP9-expressing Ctrl_1 hiPSC-Heps (Figure 5A). Analysis of mRNA (Figure 5B) and protein expression (Figure 5C) of the five UCEs showed complete absence of OTC protein in both OTCD_1 and OTCD_2 hiPSC-Heps (Figure 5C). The other UCEs were expressed at normal levels in OTCD_1 hiPSC-Heps; in OTCD_2 hiPSC-Heps, the UCE protein levels were generally lower than in Ctrl_1 and OTCD_1 hiPSC-Heps (Figure 5C). Relative OTC activity was significantly decreased in OTCD_1 and nearly absent in OTCD_2 hiPSC-Heps, respectively (Figure 5D). In accord, OTC protein expression was abundant in Ctrl_1 hiPSC-Heps but undetectable by immunofluorescence in OTCD_1 and OTCD_2 hiPSC-Heps (Figure 5E). Together, these results show that OTCD patient-derived hiPSC-Heps replicate the disease as evidenced by reduced/absent OTC expression and activity leading to impaired urea secretion.

OTC and AQP9 Co-expression Restores Ureagenesis in OTC-deficient Patient-derived hiPSC-Heps

To correct the OTCD phenotype we co-transduced patient-derived hiPSC-Heps with lentiviruses expressing OTC and AQP9. OTC expression was assessed by Western blot (Figure 6A) and analysis of OTC activity (Figure 6B) and both significantly increased upon OTC transduction. We also measured citrulline—the product of the OTC-mediated transcarbamylation of ornithine—in

cell culture supernatant. Its abundance significantly increased upon OTC expression in Ctrl_1, OTCD_1 and OTCD_2 hiPSC-Heps (Figure 6C). In accord, ureagenesis in OTCD_1 and OTCD_2 hiPSC-Heps increased significantly upon OTC transduction (Figure 6D). Whereas in OTCD_1 hiPSC-Heps ureagenesis was normalized and reached levels comparable to Ctrl_1 hiPSC-Heps, restoration was less pronounced in OTCD_2 hiPSC-Heps (Figure 6D). This deficiency was likely due to the low levels of distal UCE expression (ASS and ASL) in OTCD_2 hiPSC-Heps (Figure 5C). Thus, co-transduction of AQP9 and OTC resulted in correction of OTC expression and activity as well as in significant increases of citrulline as the direct product of the OTC reaction and ureagenesis in hiPSC-Heps from both OTCD patients.

Finally, we explored induction of endogenous AQP9 expression as a physiological alternative to lentiviral overexpression. Previous findings of a glucocorticoid-responsive element motif in the *AQP9* promoter suggest that AQP9 is regulated by the catabolic hormones glucagon and glucocorticoids (16). In accord, we found that glucagon and the potent glucocorticoid dexamethasone induce *AQP9* expression and urea secretion in hiPSC-Heps (Supporting Fig. 6A-D).

Discussion

UCDs are rare inborn errors of metabolism caused by mutations in one of the UCEs (34). Affected patients suffer from recurrent and life-threatening hyperammonemic decompensations and from severe neurological sequelae (35). In addition to the neurological phenotype found in all UCDs, involvement of the liver in form of acute organ failure or chronic hepatic disease is particularly common in OTCD (31, 36). It has been suggested that high ammonia levels contribute to acute liver failure observed in more than 50% of OTCD patients (31). In fact, acute liver failure accounts for a substantial number of deaths among OTCD patients as seen in our OTCD_2 patient (31). Current treatment strategies including dietary protein restriction, nitrogen scavengers and avoidance of catabolism are unfortunately not sufficient to fully suppress recurrent metabolic crises and the resulting morbidity (34). While another therapeutic option, liver transplantation, is curative, this approach is not only invasive but has several important limitations such as liver donor shortage and requirement of life-long immunosuppressive therapy (37). Thus, alternative strategies for the treatment of UCDs are needed especially for patients with severe disease and early life-threatening hyperammonemic crises. One such novel approach could be gene addition or gene editing, and indeed adeno-associated viruses were shown to correct OTCD in preclinical animal models (38-40) and are currently being investigated in clinical trials in adult human subjects suffering from mild OTCD (NCT02991144).

In the preclinical phase of novel treatment development, cellular or animal models of the target disease are essential, which prompted us to develop a model of OTCD based on patient-derived hiPSC-Heps. By accurately replicating the disease at the genetic and functional level, such a model would facilitate detailed analyses of patient-specific pathophysiology that could inform individual risk assessment and disease management, including genotype-phenotype correlation. In addition, a faithful *in vitro* model of OTCD could be used to identify (patient-specific) drugs by high-throughput screening.

The gold standard for determining differences in urea cycle activity in OTCD and other UCDs is to assess enrichment of secreted [^{15}N]-labeled urea after challenging cells with NH_4Cl labeled with the stable isotope [^{15}N] (26, 41). However, to be able to apply this sensitive assay to OTCD patient-derived hiPSC-Heps, we first had to address the question of why hiPSC-Heps from normal controls secrete less urea than PHHs.

Human iPSC-Heps resemble fetal rather than mature adult hepatocytes (14). Therefore, we analyzed published gene expression profiles of fetal and adult human liver tissues (21) to identify differentially expressed genes that could explain the difference in urea secretion between hiPSC-Heps and PHHs. Although some UCEs were expressed at lower levels in hiPSC-Heps than in PHHs, their activity appeared sufficient for ammonia detoxification. In contrast, we found that *AQP9*, which is required for hepatocyte urea secretion (15, 16, 29, 42-44) and virtually absent in human fetal liver tissue, is insufficiently expressed in hiPSC-Heps.

Our results demonstrate that lack of AQP9 in hiPSC-Heps causes reduced urea secretion and intracellular accumulation of urea. Overexpression of AQP9 facilitates urea secretion and normalizes the cellular response to ammonia challenge as confirmed by [^{15}N]-ureagenesis assay. Thus, normalizing AQP9 expression facilitates faithful modeling of OTCD and other UCDs in hiPSC-Heps *in vitro*. This finding has implications for other research fields since urea secretion is commonly used as a marker of hepatocyte function of hiPSC-Heps (1). To search for a potential role of AQP9 on ammonia metabolism *in vivo*, we investigated 10 human liver tissue samples from patients suffering from hyperammonemia of unknown origin. In contrast to hiPSC-Heps, AQP9 was highly expressed in all of these liver tissue samples. Moreover, no possibly pathogenic *AQP9* variants were detected in these patients or in the HGMD® Professional database (QIAGEN®) (Supporting Fig. 7). Thus, impaired *AQP9* expression is a technical limitation of hiPSC-Heps *in vitro* but not an obvious disease-causing factor in patients.

After overcoming the obstacle of reduced urea secretion in hiPSC-Heps caused by lack of AQP9 expression, we focused on developing a hiPSC-Hep-based model of OTCD. Using hiPSCs from two OTCD patients, we found that the characteristic hepatic disease phenotype of OTCD, including reduced OTC expression and activity and diminished ureagenesis, could be recapitulated in hiPSC-Heps. We also observed differences in phenotypical severity between OTCD patient-derived hiPSC-Heps, potentially reflecting the complex genetics of OTCD, including the impact of X inactivation in female patients (12, 34). In addition to low expression levels of several UCEs in hiPSC-Heps, hiPSCs from the female OTCD patient appeared more fragile during hepatocyte differentiation and contained more vacuoles suggesting cell toxicity (data not shown). We confirmed skewed X inactivation, leading to exclusive expression of the mutated *OTC* gene (45),

in hiPSC-Heps generated from two different hiPSC clones (data not shown). Thus, the severity of the OTCD phenotype in this patient—leading to death from acute liver failure at the age of 6 years—was recapitulated in our hiPSC-Hep-based disease model.

In OTCD over 400 mutations have been identified explaining the broad spectrum of disease severity (8). Many of the identified mutations are point mutations causing reduced enzyme activity. Mutated OTC protein could be stabilized by small molecule compounds functioning as pharmacological chaperones. We recently performed a high-throughput screen in a non-cellular system for compounds interacting and stabilizing human OTC protein (unpublished data). Our OTCD model using patient-derived hiPSC-Heps could be used to assess the therapeutic efficacy of the top hits from this screen.

In summary, our study identified AQP9 expression as a missing factor in urea metabolism in hiPSC-Heps. By addressing this roadblock, we established the efficacy for modeling of OTCD of hiPSCs generated from patient-derived fibroblasts, which are routinely banked in the clinical setting. Our results pave the way for studies aiming to tailor disease management to individual patients with OTCD and develop much-needed new drugs.

Acknowledgments

We thank Ljubica Caldovic (Children's National Medical Center) for sharing the rabbit anti-human OTC antibody. We thank Renata Gallagher, Simone Kurial and Feng Chen (University of California San Francisco) for their valuable input when discussing this project.

References

1. Corbett JL, Duncan SA. iPSC-Derived Hepatocytes as a Platform for Disease Modeling and Drug Discovery. Front Med 2019;6:265.
2. Matsumoto S, Haberle J, Kido J, Mitsubuchi H, Endo F, Nakamura K. Urea cycle disorders-update. J Hum Genet 2019;64:833-847.
3. Soria LR, Ah Mew N, Brunetti-Pierri N. Progress and challenges in development of new therapies for urea cycle disorders. Hum Mol Genet 2019;28:R42-R48.
4. **Lee PC, Truong B,** Vega-Crespo A, Gilmore WB, Hermann K, Angarita SA, Tang JK, et al. Restoring Ureagenesis in Hepatocytes by CRISPR/Cas9-mediated Genomic Addition to Arginase-deficient Induced Pluripotent Stem Cells. Mol Ther Nucleic Acids 2016;5:e394.
5. Yoshitoshi-Uebayashi EY, Toyoda T, Yasuda K, Kotaka M, Nomoto K, Okita K, Yasuchika K, et al. Modelling urea-cycle disorder citrullinemia type 1 with disease-specific iPSCs. Biochem Biophys Res Commun 2017;486:613-619.
6. Kim Y, Choi JY, Lee SH, Lee BH, Yoo HW, Han YM. Malfunction in Mitochondrial beta-Oxidation Contributes to Lipid Accumulation in Hepatocyte-Like Cells Derived from Citrin Deficiency-Induced Pluripotent Stem Cells. Stem Cells Dev 2016;25:636-647.
7. Summar ML, Koelker S, Freedenberg D, Le Mons C, Haberle J, Lee HS, Kirmse B, et al. The incidence of urea cycle disorders. Mol Genet Metab 2013;110:179-180.
8. Caldovic L, Abdikarim I, Narain S, Tuchman M, Morizono H. Genotype-Phenotype Correlations in Ornithine Transcarbamylase Deficiency: A Mutation Update. J Genet Genomics 2015;42:181-194.
9. Maestri NE, Lord C, Glynn M, Bale A, Brusilow SW. The phenotype of ostensibly healthy women who are carriers for ornithine transcarbamylase deficiency. Medicine 1998;77:389-397.
10. Adam S, Almeida MF, Assoun M, Baruteau J, Bernabei SM, Bigot S, Champion H, et al. Dietary management of urea cycle disorders: European practice. Mol Genet Metab 2013;110:439-445.
11. Burgard P, Kolker S, Haege G, Lindner M, Hoffmann GF. Neonatal mortality and outcome at the end of the first year of life in early onset urea cycle disorders--review and meta-analysis of observational studies published over more than 35 years. J Inherit Metab Dis 2016;39:219-229.
12. Batshaw ML, Tuchman M, Summar M, Seminara J, Members of the Urea Cycle Disorders C. A longitudinal study of urea cycle disorders. Mol Genet Metab 2014;113:127-130.

13. **Zhang S, Chen S,** Li W, Guo X, Zhao P, Xu J, Chen Y, et al. Rescue of ATP7B function in hepatocyte-like cells from Wilson's disease induced pluripotent stem cells using gene therapy or the chaperone drug curcumin. Hum Mol Genet 2011;20:3176-3187.

14. Baxter M, Withey S, Harrison S, Segeritz CP, Zhang F, Atkinson-Dell R, Rowe C, et al. Phenotypic and functional analyses show stem cell-derived hepatocyte-like cells better mimic fetal rather than adult hepatocytes. J Hepatol 2015;62:581-589.

15. Ishibashi K, Kuwahara M, Gu Y, Tanaka Y, Marumo F, Sasaki S. Cloning and functional expression of a new aquaporin (AQP9) abundantly expressed in the peripheral leukocytes permeable to water and urea, but not to glycerol. Biochem Biophys Res Commun 1998;244:268-274.

16. Tsukaguchi H, Shayakul C, Berger UV, Mackenzie B, Devidas S, Guggino WB, van Hoek AN, et al. Molecular characterization of a broad selectivity neutral solute channel. J Biol Chem 1998;273:24737-24743.

17. Okita K, Matsumura Y, Sato Y, Okada A, Morizane A, Okamoto S, Hong H, et al. A more efficient method to generate integration-free human iPS cells. Nat Methods 2011;8:409-412.

18. **Lee-Montiel FT, Laemmle A,** Charwat V, Dumont L, Lee CS, Huebsch N, Okochi H, et al. Integrated Isogenic Human Induced Pluripotent Stem Cell-Based Liver and Heart Microphysiological Systems Predict Unsafe Drug-Drug Interaction. Front Pharmacol 2021;12:667010.

19. Laemmle A, Hahn D, Hu L, Rufenacht V, Gautschi M, Leibundgut K, Nuoffer JM, et al. Fatal hyperammonemia and carbamoyl phosphate synthetase 1 (CPS1) deficiency following high-dose chemotherapy and autologous hematopoietic stem cell transplantation. Mol Genet Metab 2015;114:438-444.

20. **Schaub JR, Huppert KA, Kurial SNT,** Hsu BY, Cast AE, Donnelly B, Karns RA, et al. De novo formation of the biliary system by TGFbeta-mediated hepatocyte transdifferentiation. Nature 2018;557:247-251.

21. **Bonder MJ, Kasela S,** Kals M, Tamm R, Lokk K, Barragan I, Buurman WA, et al. Genetic and epigenetic regulation of gene expression in fetal and adult human livers. BMC Genomics 2014;15:860.

22. Berger DR, Ware BR, Davidson MD, Allsup SR, Khetani SR. Enhancing the functional maturity of induced pluripotent stem cell-derived human hepatocytes by controlled presentation of cell-cell interactions in vitro. Hepatology 2015;61:1370-1381.

23. Matz P, Wruck W, Fauler B, Herebian D, Mielke T, Adjaye J. Footprint-free human fetal foreskin derived iPSCs: A tool for modeling hepatogenesis associated gene regulatory networks. Sci Rep 2017;7:6294.
24. Wruck W, Adjaye J. Human pluripotent stem cell derived HLC transcriptome data enables molecular dissection of hepatogenesis. Sci Data 2018;5:180035.
25. **Zhu S, Rezvani M, Harbell J,** Mattis AN, Wolfe AR, Benet LZ, Willenbring H, et al. Mouse liver repopulation with hepatocytes generated from human fibroblasts. Nature 2014;508:93-97.
26. Allegri G, Deplazes S, Grisch-Chan HM, Mathis D, Fingerhut R, Haberle J, Thony B. A simple dried blood spot-method for in vivo measurement of ureagenesis by gas chromatography-mass spectrometry using stable isotopes. Clin Chim Acta 2017;464:236-243.
27. Brown GW, Jr., Cohen PP. Comparative biochemistry of urea synthesis. I. Methods for the quantitative assay of urea cycle enzymes in liver. J Biol Chem 1959;234:1769-1774.
28. Maeda N, Funahashi T, Shimomura I. Metabolic impact of adipose and hepatic glycerol channels aquaporin 7 and aquaporin 9. Nat Clin Pract Endocrinol Metab 2008;4:627-634.
29. Tsukaguchi H, Weremowicz S, Morton CC, Hediger MA. Functional and molecular characterization of the human neutral solute channel aquaporin-9. Am J Physiol 1999;277:F685-696.
30. **Hakvoort TB, He Y,** Kulik W, Vermeulen JL, Duijst S, Ruijter JM, Runge JH, et al. Pivotal role of glutamine synthetase in ammonia detoxification. Hepatology 2017;65:281-293.
31. Laemmle A, Gallagher RC, Keogh A, Stricker T, Gautschi M, Nuoffer JM, Baumgartner MR, et al. Frequency and Pathophysiology of Acute Liver Failure in Ornithine Transcarbamylase Deficiency (OTCD). PLoS One 2016;11:e0153358.
32. Tuchman M. Mutations and polymorphisms in the human ornithine transcarbamylase gene. Hum Mutat 1993;2:174-178.
33. Grompe M, Caskey CT, Fenwick RG. Improved molecular diagnostics for ornithine transcarbamylase deficiency. Am J Hum Genet 1991;48:212-222.
34. Haberle J, Burlina A, Chakrapani A, Dixon M, Karall D, Lindner M, Mandel H, et al. Suggested guidelines for the diagnosis and management of urea cycle disorders: First revision. J Inherit Metab Dis 2019;42:1192-1230.
35. Enns GM. Neurologic damage and neurocognitive dysfunction in urea cycle disorders. Semin Pediatr Neurol 2008;15:132-139.

36. Gallagher RC, Lam C, Wong D, Cederbaum S, Sokol RJ. Significant hepatic involvement in patients with ornithine transcarbamylase deficiency. J Pediatr 2014;164:720-725 e726.
37. Yu L, Rayhill SC, Hsu EK, Landis CS. Liver Transplantation for Urea Cycle Disorders: Analysis of the United Network for Organ Sharing Database. Transplant Proc 2015;47:2413-2418.
38. **Yang Y, Wang L,** Bell P, McMenamin D, He Z, White J, Yu H, et al. A dual AAV system enables the Cas9-mediated correction of a metabolic liver disease in newborn mice. Nat Biotechnol 2016;34:334-338.
39. Wang L, Bell P, Morizono H, He Z, Pumbo E, Yu H, White J, et al. AAV gene therapy corrects OTC deficiency and prevents liver fibrosis in aged OTC-knock out heterozygous mice. Mol Genet Metab 2017;120:299-305.
40. Cunningham SC, Siew SM, Hallwirth CV, Bolitho C, Sasaki N, Garg G, Michael IP, et al. Modeling correction of severe urea cycle defects in the growing murine liver using a hybrid recombinant adeno-associated virus/piggyBac transposase gene delivery system. Hepatology 2015;62:417-428.
41. Yudkoff M, Daikhin Y, Nissim I, Jawad A, Wilson J, Batshaw M. In vivo nitrogen metabolism in ornithine transcarbamylase deficiency. J Clin Invest 1996;98:2167-2173.
42. Li C, Wang W. Molecular Biology of Aquaporins. Adv Exp Med Biol 2017;969:1-34.
43. Lindskog C, Asplund A, Catrina A, Nielsen S, Rutzler M. A Systematic Characterization of Aquaporin-9 Expression in Human Normal and Pathological Tissues. J Histochem Cytochem 2016;64:287-300.
44. Litman T, Sogaard R, Zeuthen T. Ammonia and urea permeability of mammalian aquaporins. Handb Exp Pharmacol 2009:327-358.
45. Lyu C, Shen J, Zhang J, Xue F, Liu X, Liu W, Fu R, et al. The State of Skewed X Chromosome Inactivation is Retained in the Induced Pluripotent Stem Cells from a Female with Hemophilia B. Stem Cells Dev 2017;26:1003-1011.

Author names in bold designate shared co-first authorship

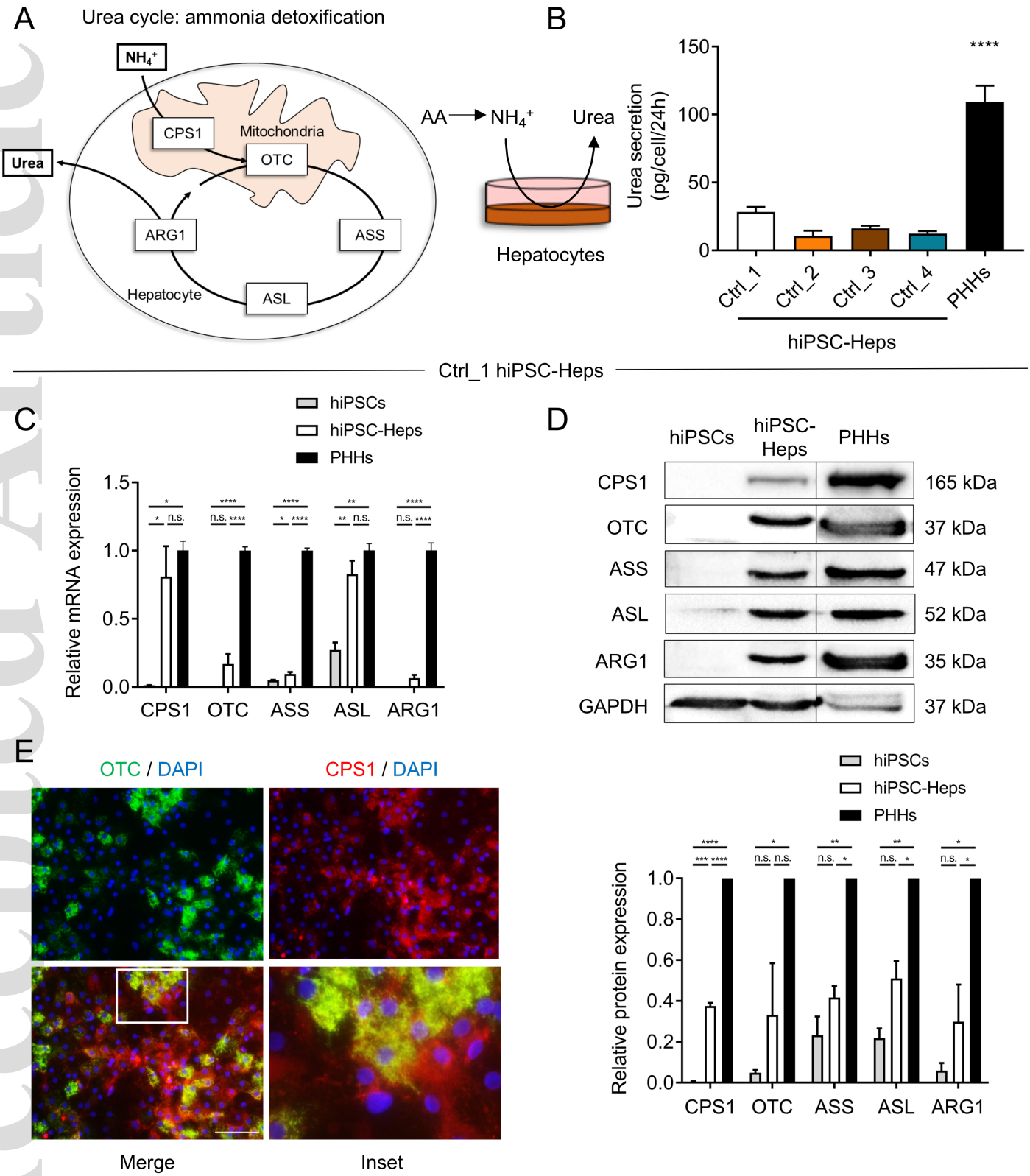

hep_32247_f1.tiff

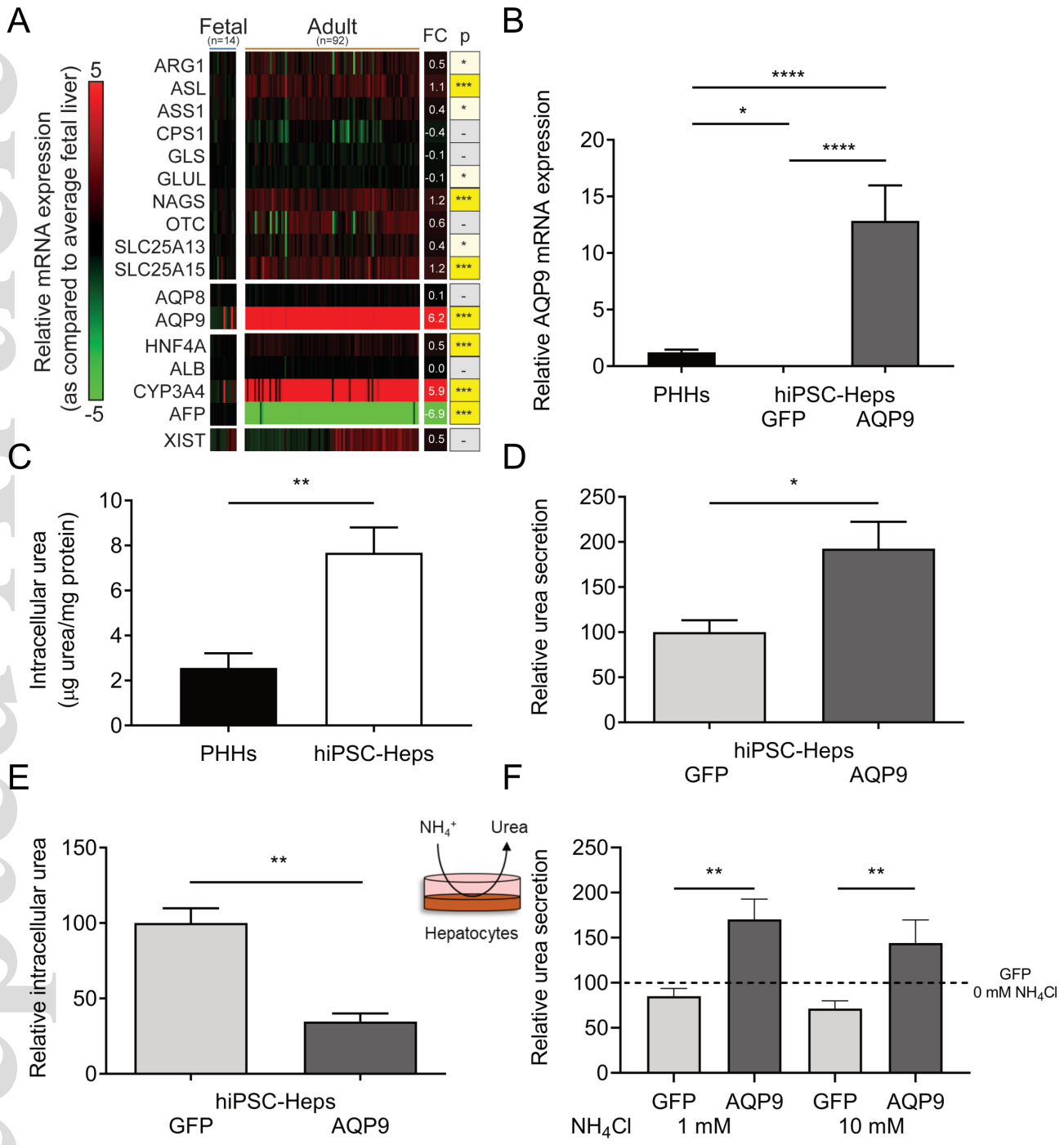

hep_32247_f2.tiff

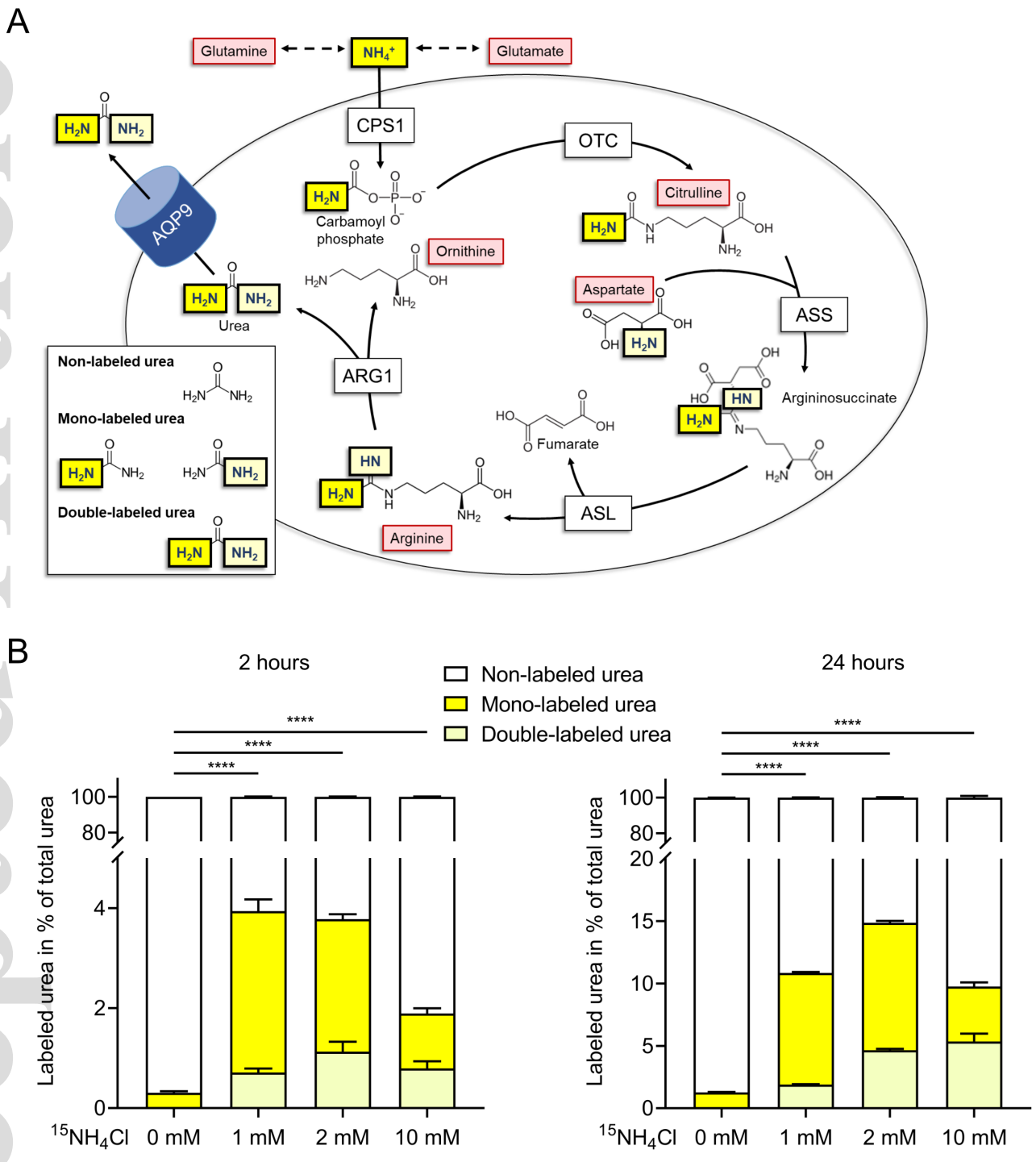

hep_32247_f3.tiff

A

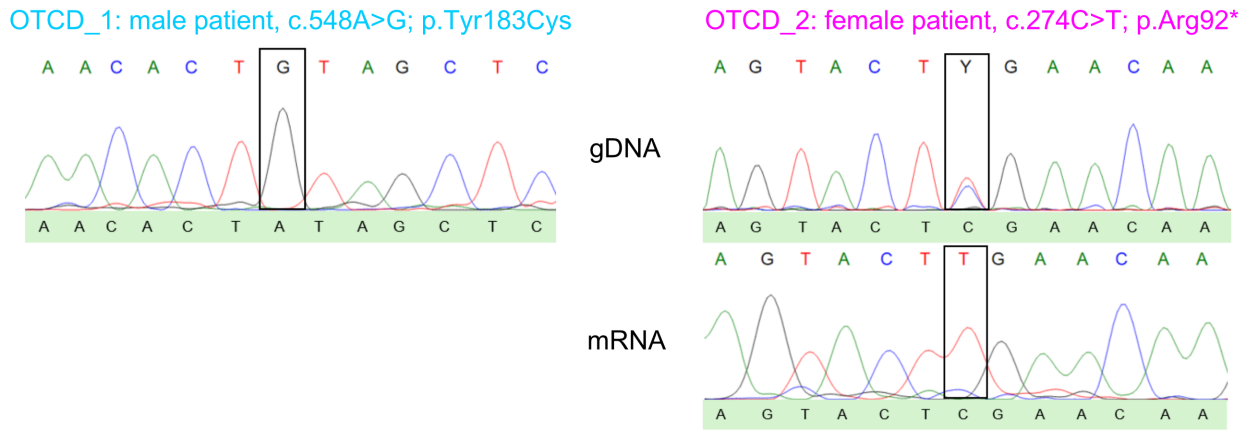

B

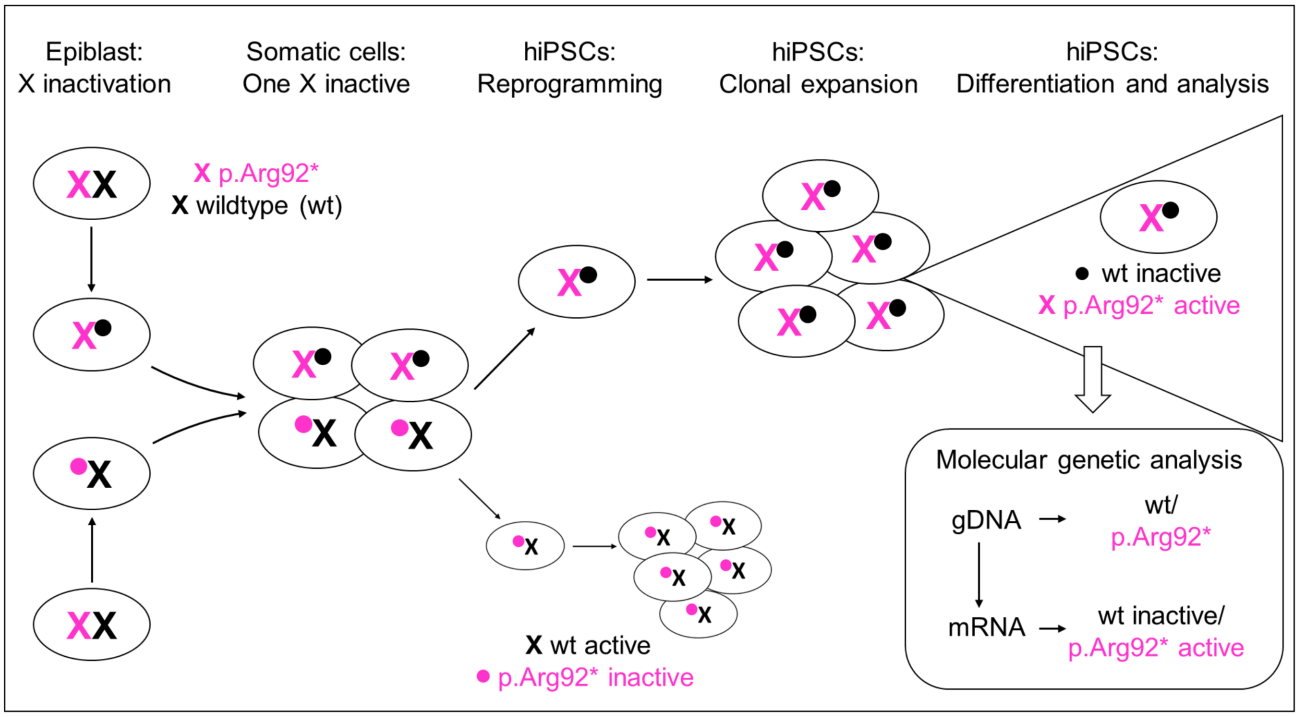

C

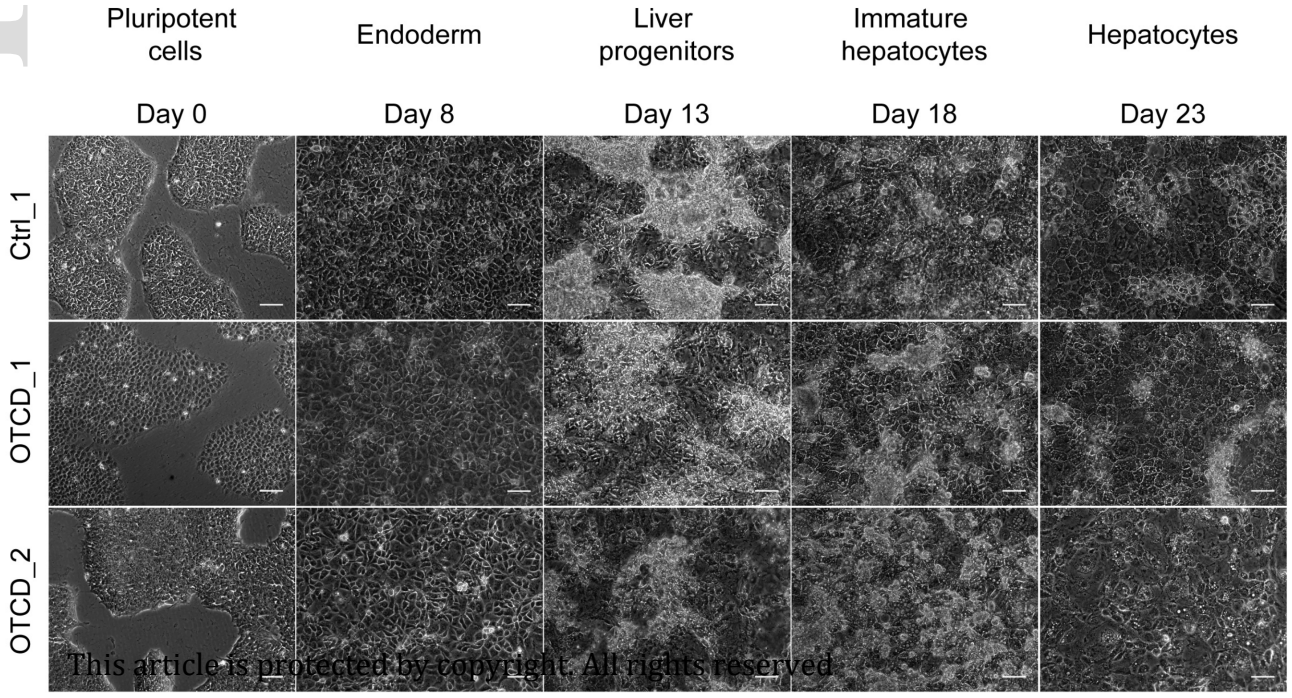

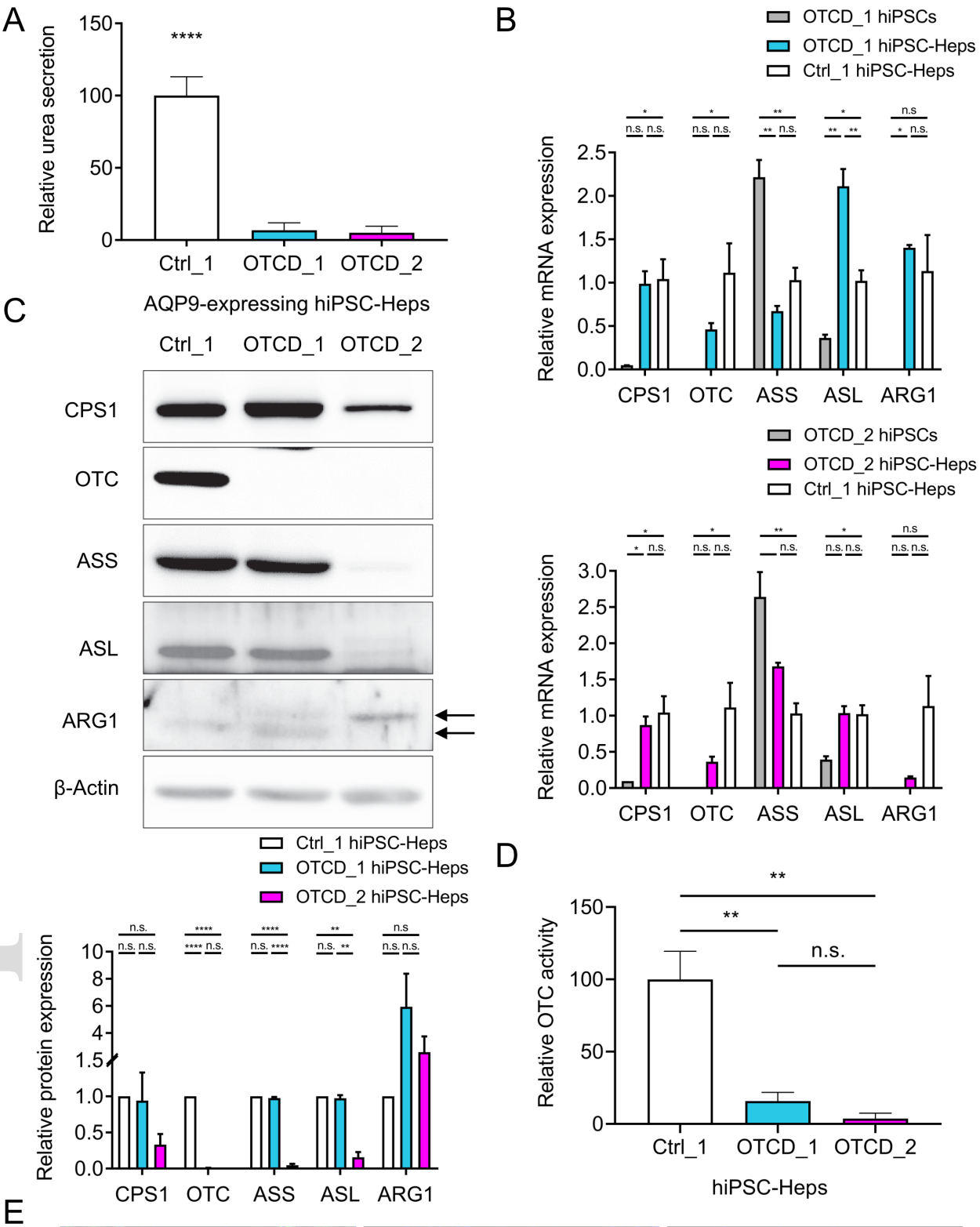

hep_32247_f5.tiff

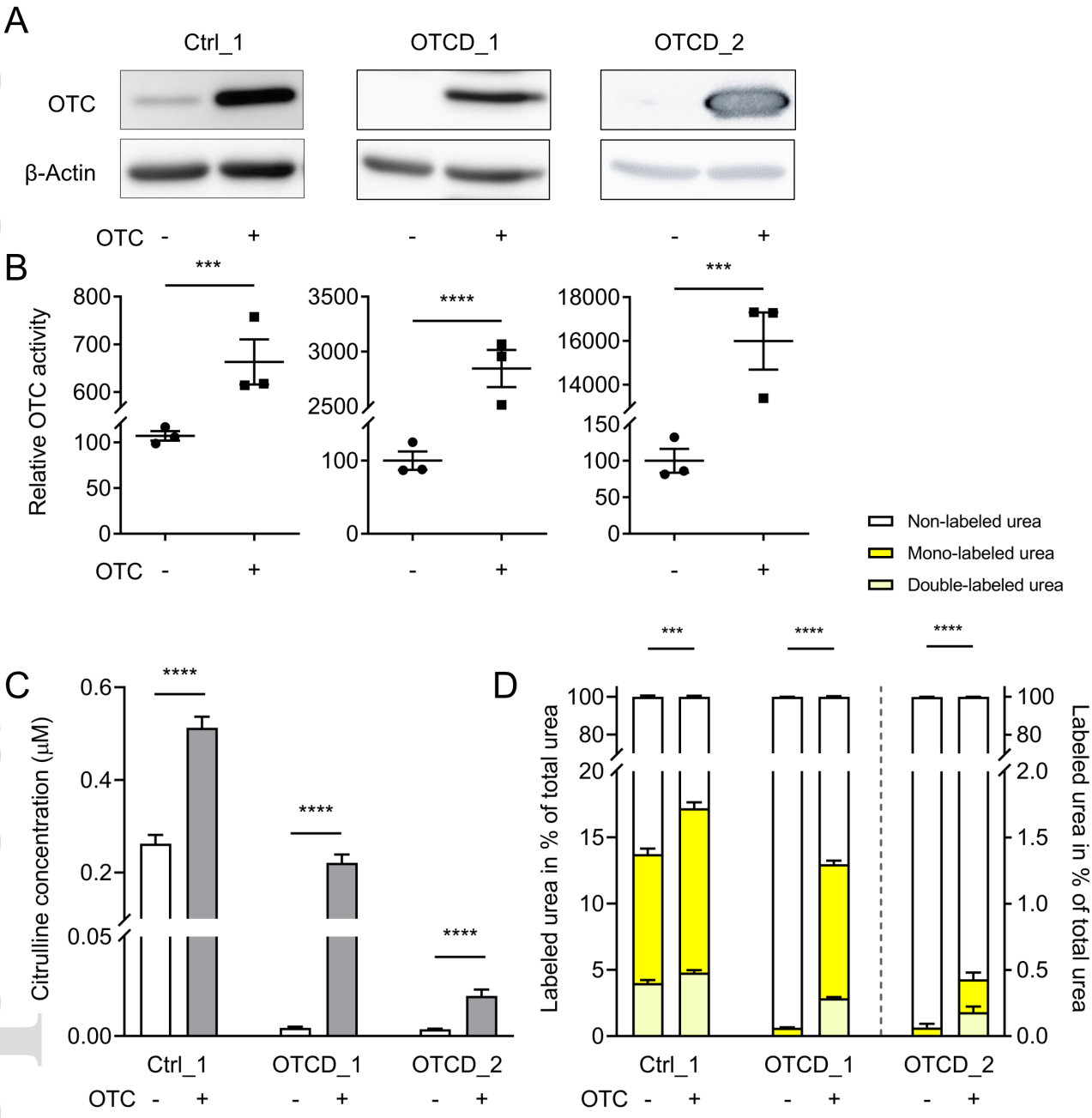

hep_32247_f6.tiff